## Measurement of the $\tau$ Neutrino Helicity and Michel Parameters in Polarized $e^+e^-$ Collisions

K. Abe, <sup>19</sup> K. Abe, <sup>30</sup> T. Akagi, <sup>28</sup> N. J. Allen, <sup>4</sup> W. W. Ash, <sup>28</sup>, \* D. Aston, <sup>28</sup> K. G. Baird, <sup>24</sup> C. Baltay, <sup>34</sup> H. R. Band, <sup>33</sup> M. B. Barakat,<sup>34</sup> G. Baranko,<sup>9</sup> O. Bardon,<sup>15</sup> T. L. Barklow,<sup>28</sup> G. L. Bashindzhagyan,<sup>18</sup> A. O. Bazarko,<sup>10</sup> R. Ben-David, <sup>34</sup> A. C. Benvenuti, <sup>2</sup> G. M. Bilei, <sup>22</sup> D. Bisello, <sup>21</sup> G. Blaylock, <sup>16</sup> J. R. Bogart, <sup>28</sup> B. Bolen, <sup>17</sup> T. Bolton, <sup>10</sup> G. R. Bower, <sup>28</sup> J. E. Brau, <sup>20</sup> M. Breidenbach, <sup>28</sup> W. M. Bugg, <sup>29</sup> D. Burke, <sup>28</sup> T. H. Burnett, <sup>32</sup> P. N. Burrows, <sup>15</sup> W. Busza, <sup>15</sup> A. Calcaterra, <sup>12</sup> D. O. Caldwell, <sup>5</sup> D. Calloway, <sup>28</sup> B. Camanzi, <sup>11</sup> M. Carpinelli, <sup>23</sup> R. Cassell, <sup>28</sup> R. Castaldi,<sup>23,†</sup> A. Castro,<sup>21</sup> M. Cavalli-Sforza,<sup>6</sup> A. Chou,<sup>28</sup> E. Church,<sup>32</sup> H. O. Cohn,<sup>29</sup> J. A. Coller,<sup>3</sup> V. Cook,<sup>32</sup> R. Cotton, R. F. Cowan, D. G. Coyne, G. Crawford, R. D'Oliveira, C. J. S. Damerell, M. Daoudi, R. Cotton, A. D. Coyne, G. Crawford, G. Crawford, R. F. Cowan, Daoudi, Control of the Country of the Count R. De Sangro, <sup>12</sup> R. Dell'Orso, <sup>23</sup> P. J. Dervan, <sup>4</sup> M. Dima, <sup>8</sup> D. N. Dong, <sup>15</sup> P. Y. C. Du, <sup>29</sup> R. Dubois, <sup>28</sup> B. I. Eisenstein, <sup>13</sup> R. Elia, <sup>28</sup> E. Etzion, <sup>33</sup> S. Fahey, <sup>9</sup> D. Falciai, <sup>22</sup> C. Fan, <sup>9</sup> J. P. Fernandez, <sup>6</sup> M. J. Fero, <sup>15</sup> R. Frey, <sup>20</sup> K. Furuno, <sup>20</sup> T. Gillman, <sup>25</sup> G. Gladding, <sup>13</sup> S. Gonzalez, <sup>15</sup> E. L. Hart, <sup>29</sup> J. L. Harton, <sup>8</sup> A. Hasan, <sup>4</sup> Y. Hasegawa, <sup>30</sup> K. Hasuko, <sup>30</sup> S. J. Hedges,<sup>3</sup> S. S. Hertzbach,<sup>16</sup> M. D. Hildreth,<sup>28</sup> J. Huber,<sup>20</sup> M. E. Huffer,<sup>28</sup> E. W. Hughes,<sup>28</sup> H. Hwang,<sup>20</sup> Y. Iwasaki, <sup>30</sup> D. J. Jackson, <sup>25</sup> P. Jacques, <sup>24</sup> J. A. Jaros, <sup>28</sup> A. S. Johnson, <sup>3</sup> J. R. Johnson, <sup>33</sup> R. A. Johnson, <sup>7</sup> T. Junk, <sup>28</sup> R. Kajikawa, <sup>19</sup> M. Kalelkar, <sup>24</sup> H. J. Kang, <sup>26</sup> I. Karliner, <sup>13</sup> H. Kawahara, <sup>28</sup> H. W. Kendall, <sup>15</sup> Y. D. Kim, <sup>26</sup> M. E. King, <sup>28</sup> R. King, <sup>28</sup> R. R. Kofler, <sup>16</sup> N. M. Krishna, <sup>9</sup> R. S. Kroeger, <sup>17</sup> J. F. Labs, <sup>28</sup> M. Langston, <sup>20</sup> A. Lath, <sup>15</sup> J. A. Lauber, <sup>9</sup> D. W. G. S. Leith, <sup>28</sup> V. Lia, <sup>15</sup> M. X. Liu, <sup>34</sup> X. Liu, <sup>6</sup> M. Loreti, <sup>21</sup> A. Lu, <sup>5</sup> H. L. Lynch, <sup>28</sup> J. Ma, <sup>32</sup> G. Mancinelli, <sup>22</sup> S. Manly, <sup>34</sup> G. Mantovani, <sup>22</sup> T. W. Markiewicz, <sup>28</sup> T. Maruyama, <sup>28</sup> H. Masuda, <sup>28</sup> E. Mazzucato, <sup>11</sup> A. K. McKemey, <sup>4</sup> B. T. Meadows, <sup>7</sup> R. Messner, <sup>28</sup> P. M. Mockett, <sup>32</sup> K. C. Moffeit, <sup>28</sup> T. B. Moore, <sup>34</sup> D. Muller, <sup>28</sup> T. Nagamine, <sup>28</sup> S. Narita,<sup>30</sup> U. Nauenberg,<sup>9</sup> H. Neal,<sup>28</sup> M. Nussbaum,<sup>7</sup> Y. Ohnishi,<sup>19</sup> L. S. Osborne,<sup>15</sup> R. S. Panvini,<sup>31</sup> C. H. Park,<sup>27</sup> H. Park, <sup>20</sup> T. J. Pavel, <sup>28</sup> I. Peruzzi, <sup>12,‡</sup> M. Piccolo, <sup>12</sup> L. Piemontese, <sup>11</sup> E. Pieroni, <sup>23</sup> K. T. Pitts, <sup>20</sup> R. J. Plano, <sup>24</sup> R. Prepost, <sup>33</sup> C. Y. Prescott, <sup>28</sup> G. D. Punkar, <sup>28</sup> J. Quigley, <sup>15</sup> B. N. Ratcliff, <sup>28</sup> T. W. Reeves, <sup>31</sup> J. Reidy, <sup>17</sup> P. L. Reinertsen, P. E. Rensing, L. S. Rochester, P. C. Rowson, U. J. J. Russell, O. H. Saxton, T. Schalk, G. R. H. Schindler, <sup>28</sup> B. A. Schumm, <sup>6</sup> S. Sen, <sup>34</sup> V. V. Serbo, <sup>33</sup> M. H. Shaevitz, <sup>10</sup> J. T. Shank, <sup>3</sup> G. Shapiro, <sup>14</sup> D. J. Sherden, <sup>28</sup> K. D. Shmakov, <sup>29</sup> C. Simopoulos, <sup>28</sup> N. B. Sinev, <sup>20</sup> S. R. Smith, <sup>28</sup> M. B. Smy, <sup>8</sup> J. A. Snyder, <sup>34</sup> P. Stamer,<sup>24</sup> H. Steiner,<sup>14</sup> R. Steiner,<sup>1</sup> M. G. Strauss,<sup>16</sup> D. Su,<sup>28</sup> F. Suekane,<sup>30</sup> A. Sugiyama,<sup>19</sup> S. Suzuki,<sup>19</sup> M. Swartz, <sup>28</sup> A. Szumilo, <sup>32</sup> T. Takahashi, <sup>28</sup> F. E. Taylor, <sup>15</sup> E. Torrence, <sup>15</sup> A. I. Trandafir, <sup>16</sup> J. D. Turk, <sup>34</sup> T. Usher, <sup>28</sup> J. Va'vra, <sup>28</sup> C. Vannini, <sup>23</sup> E. Vella, <sup>28</sup> J. P. Venuti, <sup>31</sup> R. Verdier, <sup>15</sup> P. G. Verdini, <sup>23</sup> D. L. Wagner, <sup>9</sup> S. R. Wagner, <sup>28</sup> A. P. Waite, <sup>28</sup> S. J. Watts, <sup>4</sup> A. W. Weidemann, <sup>29</sup> E. R. Weiss, <sup>32</sup> J. S. Whitaker, <sup>3</sup> S. L. White, <sup>29</sup> F. J. Wickens, <sup>25</sup> D. A. Williams, D. C. Williams, S. H. Williams, S. Willocq, R. J. Wilson, W. J. Wisniewski, M. Woods, M. Woods, 28 G.B. Word,<sup>24</sup> J. Wyss,<sup>21</sup> R. K. Yamamoto,<sup>15</sup> J. M. Yamartino,<sup>15</sup> X. Yang,<sup>20</sup> J. Yashima,<sup>30</sup> S. J. Yellin,<sup>5</sup> C. C. Young, <sup>28</sup> H. Yuta, <sup>30</sup> G. Zapalac, <sup>33</sup> R. W. Zdarko, <sup>28</sup> and J. Zhou<sup>20</sup>

## (The SLD Collaboration)

<sup>1</sup>Adelphi University, Garden City, New York 11530 <sup>2</sup>INFN Sezione di Bologna, I-40126 Bologna, Italy <sup>3</sup>Boston University, Boston, Massachusetts 02215 <sup>4</sup>Brunel University, Uxbridge, Middlesex UB8 3PH, United Kingdom <sup>5</sup>University of California at Santa Barbara, Santa Barbara, California 93106 <sup>6</sup>University of California at Santa Cruz, Santa Cruz, California 95064 <sup>7</sup>University of Cincinnati, Cincinnati, Ohio 45221 <sup>8</sup>Colorado State University, Fort Collins, Colorado 80523 <sup>9</sup>University of Colorado, Boulder, Colorado 80309 <sup>10</sup>Columbia University, New York, New York 10027 <sup>11</sup>INFN Sezione di Ferrara and Università di Ferrara, I-44100 Ferrara, Italy <sup>12</sup>INFN Lab. Nazionali di Frascati, I-00044 Frascati, Italy <sup>13</sup>University of Illinois, Urbana, Illinois 61801 <sup>14</sup>Lawrence Berkeley Laboratory, University of California, Berkeley, California 94720 <sup>15</sup>Massachusetts Institute of Technology, Cambridge, Massachusetts 02139 <sup>16</sup>University of Massachusetts, Amherst, Massachusetts 01003 <sup>17</sup>University of Mississippi, University, Mississippi 38677 <sup>18</sup>Moscow State University, Institute of Nuclear Physics, 119899 Moscow, Russia <sup>19</sup>Nagoya University, Chikusa-ku, Nagoya 464 Japan <sup>20</sup>University of Oregon, Eugene, Oregon 97403

21 INFN Sezione di Padova and Università di Padova, I-35100 Padova, Italy
 22 INFN Sezione di Perugia and Università di Perugia, I-06100 Perugia, Italy
 23 INFN Sezione di Pisa and Università di Pisa, I-56100 Pisa, Italy
 24 Rutgers University, Piscataway, New Jersey 08855
 25 Rutherford Appleton Laboratory, Chilton, Didcot Oxon OX11 0QX, United Kingdom
 26 Sogang University, Seoul, Korea
 27 Soongsil University, Seoul, Korea 156-743
 28 Stanford Linear Accelerator Center, Stanford University, Stanford, California 94309
 29 University of Tennessee, Knoxville, Tennessee 37996
 30 Tohoku University, Sendai 980 Japan
 31 Vanderbilt University, Nashville, Tennessee 37235
 32 University of Washington, Seattle, Washington 98195
 33 University of Wisconsin, Madison, Wisconsin 53706
 34 Yale University, New Haven, Connecticut 06511
 (Received 31 January 1997)

We present a new measurement of the  $\tau$  neutrino helicity  $h_{\nu_{\tau}}$  and the  $\tau$  Michel parameters  $\rho$ ,  $\eta$ ,  $\xi$ , and the product  $\delta \xi$ . The analysis exploits the highly polarized SLC electron beam to extract these quantities directly from a measurement of the  $\tau$  decay spectra, using the 1993–1995 SLD data sample of 4328  $e^+e^- \to Z^0 \to \tau^+\tau^-$  events. From the decays  $\tau \to \pi \nu_{\tau}$  and  $\tau \to \rho \nu_{\tau}$  we obtain a combined value  $h_{\nu_{\tau}} = -0.93 \pm 0.10 \pm 0.04$ . The leptonic decay channels yield combined values of  $\rho = 0.72 \pm 0.09 \pm 0.03$ ,  $\xi = 1.05 \pm 0.35 \pm 0.04$ , and  $\delta \xi = 0.88 \pm 0.27 \pm 0.04$ . [S0031-9007(97)03314-0]

PACS numbers: 13.35.Dx, 12.15.Ji, 13.88.+e, 14.60.Fg

We present a study of the fundamental structure of the charged weak current by investigating the energy spectra of decay products of polarized  $\tau$  leptons at the  $Z^0$  resonance. We measure the  $\tau$  neutrino helicity and decay Michel parameters, which are related [1,2] to the couplings in  $W \to \tau \nu_{\tau}$ . The  $\tau$  decay spectra are determined by the nature of the decay [3] and the spin polarization of the taus.

Tau pairs are produced with high longitudinal polarization in collisions of highly polarized electrons with positrons at the SLC.

In  $e^+e^- \rightarrow \tau^+\tau^-$ , final state  $\tau$  polarization results both from incident beam polarization and from parity violation of the  $Z^0$  couplings. Neglecting  $\gamma$  exchange and  $\gamma - Z^0$  interference, we can write the  $\tau$  polarization as

$$P_{\tau}(\cos\theta, P_e) \equiv \frac{d\sigma_R/d\cos\theta - d\sigma_L/d\cos\theta}{d\sigma_R/d\cos\theta + d\sigma_L/d\cos\theta} = -\frac{A_{\tau}(1 + \cos^2\theta) + 2\cos\theta(A_e - P_e)/(1 - A_eP_e)}{(1 + \cos^2\theta) + 2\cos\theta A_{\tau}(A_e - P_e)/(1 - A_eP_e)}, \quad (1)$$

where  $\theta$  is the polar angle of the  $\tau^-$  ( $\tau^+$ ) with respect to the incident  $e^-$  ( $e^+$ ) direction,  $P_e$  is the  $e^-$  beam polarization, and  $A_e$  and  $A_{\tau}$  [4] are the  $e^-$  and  $\tau$ parity-violation asymmetry parameters. This expression is plotted in Fig. 1 for  $P_e = 0$  and  $\pm 0.8$ . Experiments without beam polarization have relied on spin correlations between the final state taus [5-8] for measuring the magnitude of the parameters described above, or the hadronic structure function to measure both the magnitude and the sign of  $h_{\nu_{\tau}}$  [9,10]. At the SLC,  $P_{\tau}$  is largely determined by the beam polarization and the production angle, as seen in Fig. 1. Therefore, this allows a direct measurement using all individual identified  $\tau$  decays and, unlike the correlation methods, provides the sign as well as the magnitude of all the polarization-dependent parameters. This is the first such measurement to be performed with polarized beams.

We study the energy spectra of pions, rho mesons, electrons, and muons from  $\tau$  decays. In the case of a two-body decay, such as  $\tau \to \pi \nu_{\tau}$  or  $\tau \to \rho \nu_{\tau}$ , the decay spectrum in the  $\tau$  rest frame is monoenergetic, so the boosted energy of the  $\pi$  or  $\rho$  meson directly reflects the rest frame decay angle. In the case of a three-body decay,

such as  $\tau \to \mu \overline{\nu}_{\mu} \nu_{\tau}$  or  $\tau \to e \overline{\nu}_{e} \nu_{\tau}$ , the boosted lepton energy reflects both the decay angle and energy in the rest frame. In all cases, we can express the laboratory energy spectrum in two parts, a polarization-independent part and a part that changes sign depending on the handedness of the  $\tau$ :  $d\Gamma(z, P_{\tau}) \propto [f(z) + \zeta P_{\tau} g(z)] dz$ .

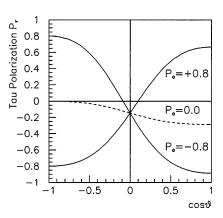


FIG. 1.  $\tau$  polarization vs production angle with and without  $e^-$  beam polarization.

High  $P_e$  provides enhanced sensitivity to the polarization-dependent parameters.

For the  $\tau \to \pi \nu_{\tau}$  mode, z is the pion energy scaled by the  $\tau$  energy ( $z = E_{\pi}/E_{\tau}$ ), and f(z) and g(z) are given by

$$f_{\pi}(z) = 1,$$
  $g_{\pi}(z) = \frac{2z - 1 - m_{\pi}^2 / m_{\tau}^2}{1 - m_{\pi}^2 / m_{\tau}^2},$  (2)

and  $\zeta$  can be interpreted as  $h_{\nu_{\tau}}$ , the helicity of the  $\nu_{\tau}$ . The  $\rho$  meson can exist in one of two helicity states. In order not to reduce the sensitivity in the  $\tau \to \rho \nu_{\tau}$  decay mode, it is necessary to spin analyze the  $\rho$ -meson decay products, as discussed in Refs. [11,12]. Thus z represents a set of three variables:  $\theta^*$ , the decay angle of the  $\rho$  meson in the  $\tau$  rest frame;  $\psi$ , the decay angle of the charged  $\pi$  in the  $\rho$ -meson rest frame; and  $m_{\rho}$ , the mass of the  $\rho$  meson. In the following we use for the  $\tau \to \rho \nu_{\tau}$  decays the notation introduced in Ref. [13],  $d\Gamma \propto [1 + \zeta P_{\tau} \omega(\theta^*, \psi, m_{\rho})] d\omega$ , where  $\omega(\theta^*, \psi, m_{\rho})$  is the ratio between the polarization-dependent term and the polarization-independent term.

In the case of the lepton decay modes, we can describe the energy spectrum with the Michel parameters [14]  $\rho$ ,  $\eta$ ,  $\xi$ , and  $\delta \xi$ . These parameters were originally conceived to describe  $\mu$  decay. They describe the energy and angular spectra of the resultant lepton with respect to the initial parent spin direction. Here the parameters  $\rho$  and  $\eta$  appear in the polarization-independent term, while  $\xi$  and  $\delta \xi$  describe the polarization-dependent behavior. Terms proportional to  $m_{\ell}^2/E_{\tau}^2$  may be neglected. Then with  $z = E_{\ell}/E_{\tau}$ , we obtain the following spectrum for  $\tau \to \ell \overline{\nu}_{\ell} \nu_{\tau}$ :

$$f_{\ell}(z) = 2 - 6z^{2} + 4z^{3} + \rho \frac{4}{9} (-1 + 9z^{2} - 8z^{3})$$

$$+ \eta \frac{m_{\ell}}{m_{\tau}} (12 - 24z + 12z^{2}),$$

$$\zeta g_{\ell}(z) = \xi \left( -\frac{2}{3} + 4z - 6z^{2} + \frac{8}{3}z^{3} \right)$$

$$+ \delta \xi \frac{4}{9} (1 - 12z + 27z^{2} - 16z^{3}).$$
(3)

These decay spectra are combined with the production cross sections to yield inclusive distributions which can be written as

$$\frac{1}{\sigma} \frac{d^2 \sigma(z, \cos \theta, P_e)}{dz d \cos \theta} \propto f(z) + \zeta P_{\tau}(\cos \theta, P_e) g(z). \tag{4}$$

For  $\tau^+$  decays, the sign of the polarization-dependent term is reversed due to the opposite helicity of the antineutrino. The normalization  $\sigma$  in general depends on the decay parameters.

The results reported here are based on the data collected by SLD during the period 1993–1995 at a center of mass energy of 91.2 GeV. The 1993 run accumulated an integrated luminosity of 1.78 pb<sup>-1</sup> with an average  $e^-$  beam polarization of  $(63.0 \pm 1.1)\%$ , and the 1994–1995 run

accumulated  $3.66 \text{ pb}^{-1}$  with an average polarization of  $(77.2 \pm 0.5)\%$ . A general description of the SLD can be found elsewhere ([15], and references therein). Charged particle tracking and momentum analysis are provided by the central drift chamber (CDC) and the charge-coupled device (CCD)-based vertex detector (VXD) in an axial magnetic field of 0.6 T. Particle energies are measured in the liquid argon calorimeter (LAC), which is segmented into projective towers with separate electromagnetic (EM) and hadronic sections. The measured energy and the shape of the energy flow are used for particle identification. Additional particle identification is provided by the Čerenkov ring-imaging detector (CRID), and muons are identified in the warm iron calorimeter (WIC).

The initial selection of  $\tau$ -pair candidates is based on the multiplicity, momentum, and direction of tracks in the CDC, and on properties of EM showers in the calorimeter, resulting in a sample of 4328 events with a purity of 98% and an efficiency of 80% in the fiducial region  $|\cos \theta|$ 0.74. The background contamination and efficiency of the event selection and decay identification (described below) were estimated and parametrized using a Monte Carlo (MC) simulation. Details on the event selection and simulation are given in Ref. [15]. These events are divided into hemispheres by the plane normal to the event thrust axis, and the hemispheres are treated independently. Any pair of oppositely charged tracks which is consistent with originating from a  $\gamma$  conversion is removed. Hemispheres are then required to contain exactly one track, and the track is required to have at least one hit in the VXD to improve momentum resolution.

The selection of  $\tau \to \mu \overline{\nu}_{\mu} \nu_{\tau}$  in the region  $|\cos \theta| < 0.62$  is performed by associating WIC hits with CDC tracks. In the region  $0.62 < |\cos \theta| < 0.74$ , shower information from the LAC is used instead. A minimum track momentum of 1.6 GeV/c is required. This results in a sample of 1143 tracks identified as muons, with an estimated selection efficiency of 72% within the acceptance, and an estimated purity of 94%. The background comes from  $\mu$  pairs (2%),  $2\gamma$  events (0.8%), and misidentified  $\tau$  decays (3.2%).

For selection of  $\tau \to e \overline{\nu}_e \nu_\tau$  the LAC energy deposition must be consistent with that of an electron, or the electron must be identified by the CRID. The momentum of the track must be greater than 1.6 GeV/c, and a quasi-invariant mass calculated using track momentum and LAC energy clusters is required to be less than 0.5 GeV/ $c^2$ . This results in a sample of 948 identified electron tracks with an estimated efficiency of 63% within the acceptance and an estimated purity of 96.4%. The background to this mode is composed of Bhabha and  $2\gamma$  events and misidentified  $\tau$  decays at the levels of 0.8%, 0.8%, and 2%, respectively.

For the  $\tau \to \pi \nu_{\tau}$  selection, we first reject electron and  $\mu$  candidates. Then a candidate is required to have track momentum greater than  $3~{\rm GeV}/c$ , and no EM clusters within  $10^{\circ}$  of the thrust axis that are not associated with

a CDC track. Here the calculated quasi-invariant mass is required to be less than 0.3 GeV/ $c^2$ , and additional criteria are imposed based on the ratio of LAC energy to track momentum. No attempt is made to separate kaons from pions, and a small correction is made in the analysis for the effect of the larger kaon mass. This selection provides a sample of 558 tracks identified as  $\tau \to \pi \nu_{\tau}$ , with an efficiency of 58% within the angular acceptance. The purity of the sample is approximately 79% where the main contamination sources are  $\rho$ -meson, e, and  $\mu$  decay channels at the rates of 13%, 5%, and 1.4%, respectively. The non-tau background is estimated to be less than 0.5%.

Events not selected as leptons or pions are candidates for  $\tau \to \rho \nu_{\tau}$  decays. Hemispheres are then categorized according to the number of EM clusters found within 20° of the event thrust axis, and according to whether such clusters are associated or unassociated with the charged track in the corresponding hemisphere. The charged track momentum and the EM cluster energies are used to calculate a  $\rho$ -meson energy and its invariant mass, and the mass is required to fall in the range between 0.44 and 1.2  $\text{GeV}/c^2$ . This selection results in a sample of 1295 identified  $\rho$ -meson decays, with an efficiency of 60% over the fiducial region. The purity of the sample is approximately 76%, where the background is dominated by decays to  $\pi 2\pi^{\circ}$  (14.7%),  $K^{*}$  (2.4%), and single  $\pi$  or K (2.4%). The non-tau background is estimated to be less than 0.3%.

In Fig. 2(a), the energy spectrum of  $\tau \to \pi \nu_{\tau}$  decays is plotted separately for different combinations of the production angle and the sign of  $P_e$ . For left-handed incident  $e^-$  and  $\tau^-$  emitted at forward polar angles, or for right-handed beam and  $\tau^-$  in the backward region, the  $\tau^-$  are predominantly left handed and the  $\pi$  energy spectrum is expected to be relatively soft. For the two opposite combinations of  $P_e$  and  $\cos\theta$ , the spectrum should be harder since the decaying  $\tau^-$  are predominantly right handed. Figure 2(c) shows the same comparison for the  $\tau \to \rho \nu_{\tau}$  decays. The difference is expected to be less obvious for the three-body decays  $\tau \to \ell \overline{\nu}_{\ell} \nu_{\tau}$ , but is still quite visible in Fig. 2(b). These plots also demonstrate the good agreement between data and MC, as well as the low and helicity-symmetric backgrounds.

The  $\nu_{\tau}$  helicity and the Michel parameters  $\rho$ ,  $\eta$ ,  $\xi$ , and  $\delta \xi$  are determined using a maximum likelihood fit to the  $\tau$  production angle and the energy spectra of the decay channels  $\tau \to \pi \nu_{\tau}$  and  $\tau \to \ell \overline{\nu}_{\ell} \nu_{\tau}$  ( $\omega$  spectrum for  $\tau \to \rho \nu_{\tau}$ ). The following expression is minimized:

$$W = -2\sum_{\text{decays}} \ln \left\{ \frac{1}{\sigma} \frac{d^2 \sigma}{d \cos \theta dz} \right\}.$$
 (5)

The sum in Eq. (5) runs over all  $\tau \to e \overline{\nu}_e \nu_\tau$ ,  $\tau \to \mu \overline{\nu}_\mu \nu_\tau$ ,  $\tau \to \rho \nu_\tau$ , or  $\tau \to \pi \nu_\tau$  candidates. The fit function includes effects of  $\gamma$  exchange and  $\gamma - Z^0$  interference, radiation, detector resolution, efficiency, and backgrounds. The dependence of MC efficiencies and

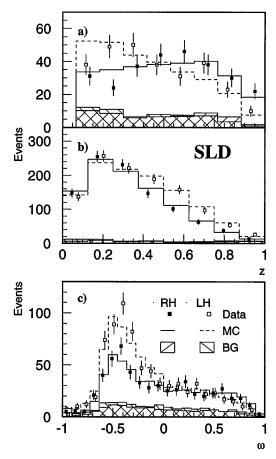


FIG. 2. (a)  $\tau \to \pi \nu_{\tau}$ , (b)  $\tau \to \ell \overline{\nu}_{\ell} \nu_{\tau}$ , and (c)  $\tau \to \rho \nu_{\tau}$  decay spectra. The solid squares (line) represent the sum of the measured (MC) spectra for  $\tau$  decays in the forward direction with  $P_e < 0$  and in the backward direction with  $P_e > 0$ , and the open squares (dashed line) are the measured (MC) sum of the spectra for  $\tau$  decays in the backward direction with  $P_e < 0$  and in the forward direction with  $P_e > 0$ . The hatched regions represent the estimated backgrounds in the two combinations. The MC was generated with the SM values for the  $\tau$  decay parameters.

backgrounds on z ( $\omega$ ) and  $\cos \theta$  is parametrized using low order polynomials. The effect of initial and final state radiation is determined from the ratio of the spectrum for MC events generated using KORALZ 4.0 [16] (including radiation) to the spectrum for the Born level cross sections. Effects of detector resolution are studied using MC for each input variable (i.e., track momentum or  $\omega$ , and  $\tau$  direction). Fits to multiple Gaussians are performed

TABLE I. Systematic uncertainties (in units of  $10^{-2}$ ).

	$h^\pi_ u$	$h^{ ho}_{ u}$	$ ho^{\it e}$	$ ho^{\mu}$	$\eta^{\mu}$	$\boldsymbol{\xi}^e$	$\xi^{\mu}$	$\delta \xi^e$	$\delta \xi^{\mu}$
Selection	0.7	2.7	2.7	4.5	13.8	2.6	4.3	4.4	2.0
Background	1.1	1.3	1.2	13.3	41.7	1.1	13.1	0.7	6.3
K fraction	0.8								
Rad. corr.	0.5	0.4	0.4	0.4	0.8	0.2	0.1	0.2	0.1
Resolution	1.3	1.5	3.8	2.6	5.1	4.9	2.2	5.9	2.9
Beam $P_e$	0.9	0.6	1.6	0.4	4.5	0.9	2.1	0.7	0.4
$A_e, A_{\tau}$ [4]	0.7	0.8	0.3	0.2	1.4	1.6	2.4	1.6	0.8
TOTAL	2.4	3.5	5.1	14.3	44.5	5.9	14.4	7.6	7.2

TABLE II. The measured  $h_{\nu_{\tau}}$  and Michel parameters including statistical and systematic errors, given by decay channel and as combined results, compared with the standard model (SM) predictions.

	SM	$ au  ightarrow \pi  u_{ au}$	$\tau \to \rho  \nu_{\tau}$	Hadrons combined
$h_{ u_{ au}}$	-1	$-0.81 \pm 0.17 \pm 0.02$	$-0.99 \pm 0.12 \pm 0.04$	$-0.93 \pm 0.10 \pm 0.04$
		$ au  ightarrow e \overline{ u}_e  u_ au$	$ au  ightarrow \mu \overline{ u}_{\mu}  u_{ au}$	$ au  ightarrow \ell \overline{ u}_\ell  u_ au$ combined
ho	$\frac{3}{4}$	$0.71 \pm 0.14 \pm 0.05$	$0.54 \pm 0.28 \pm 0.14$	$0.72 \pm 0.09 \pm 0.03$
$\eta$	0		$-0.59 \pm 0.82 \pm 0.45$	
ξ	1	$1.16 \pm 0.52 \pm 0.06$	$0.75 \pm 0.50 \pm 0.14$	$1.05 \pm 0.35 \pm 0.04$
δξ	<u>3</u> 4	$0.85 \pm 0.43 \pm 0.08$	$0.82 \pm 0.32 \pm 0.07$	$0.88 \pm 0.27 \pm 0.04$

to model both the core and tails of the resolution distributions, and these functions are convoluted with the theoretical expression. Since the spectra are different for decays of left- and right-handed taus, all the correction functions are divided into four categories corresponding to combinations of positive or negative  $e^-$  beam polarization and the forward or backward half of the detector. In all cases the analytic functions are required to be good representations of the MC distributions.

These measurements are dominated by statistical errors. Table I summarizes the systematic errors. To investigate these, the parametrizations described above are modified by their uncertainties as determined from the MC, the fit is redone to obtain new values of  $h_{\nu_{\tau}}$ ,  $\rho$ ,  $\eta$ ,  $\xi$ , and  $\delta \xi$ , and changes in the fitted values are taken as the systematic errors. The validity of these errors has been checked by comparing data and MC distributions, for example, of cluster energies, number of associated and unassociated clusters, and  $\pi^0$  and  $\rho$ -meson reconstructed masses. The observed number of events and the calculated efficiencies and backgrounds are consistent with measured branching ratios [2]. The uncertainty in the fraction of kaons in the  $\tau \to \pi \nu_{\tau}$  sample affects the correction for the kaon mass. The errors on radiative corrections are dominated by MC statistics. The beam polarization uncertainties are as quoted above. Each error listed in Table I may include several related contributions. These errors are combined taking into account any correlation between the input parameters.

The measured values for  $h_{\nu_{\tau}}$  and the Michel parameters  $\rho$ ,  $\eta$ ,  $\xi$ , and  $\delta \xi$  are given in Table II. For the combined  $\tau \to \ell \overline{\nu}_{\ell} \nu_{\tau}$  fit the correlation coefficients are  $C_{\rho-\xi}=0.06$ ,  $C_{\rho-\delta \xi}=0.03$ , and  $C_{\xi-\delta \xi}=0.08$ , while for  $\tau \to \mu \overline{\nu}_{\mu} \nu_{\tau}$  the  $\eta^{\mu}$  and  $\rho^{\mu}$  parameters are highly correlated (0.92). Note that  $\eta$  could not be measured separately for  $\tau \to e \overline{\nu}_{e} \nu_{\tau}$  due to the small  $m_{e}/m_{\tau}$  term. One could improve the  $\eta$  measurement by including the  $\tau \to e \overline{\nu}_{e} \nu_{\tau}$  data and assuming universal couplings for e and e in the charged current. In this case we get e = 0.69 e 0.13 e 0.05, e = -0.13 e 0.47 e 0.15, e = 1.02 e 0.36 e 0.05, and e = 0.87 e 0.27 e 0.04. However, this assumption is inconsistent because generally a nonzero value for e would imply e to be nonuniversal [1].

The results are consistent with the V-A predictions and are in good agreement with other experimental results [5-10]. This is the first measurement using beam polarization, and we have measured not only the magnitude but also the sign of all pseudoscalar and parity violating quantities. Because of the unique method, significant new measurements have been derived from a relatively small number of events. One can also interpret the results from leptonic decay channels [17] as  $h_{\nu_{\tau}}^{\text{leptons}} = -0.96 \pm 0.19 \pm 0.03$ , and combined with the hadronic decay channels one obtains  $h_{\nu_{\tau}}^{\text{lept}+\text{had}} = -0.94 \pm 0.09 \pm 0.03$ .

We thank the personnel of the SLAC accelerator department and the technical staffs of our collaborating institutions for their outstanding efforts on our behalf. This work was supported by the U.S. Department of Energy and National Science Foundation, the UK Particle Physics and Astronomy Research Council, the Istituto Nazionale di Fisica Nucleare of Italy, the Japan-U.S. Cooperative Research Project on High Energy Physics, and the Korea Science and Engineering Foundation.

<sup>\*</sup>Deceased.

<sup>&</sup>lt;sup>†</sup>Also at the Università di Genova, I-16146, Genova, Italy. <sup>‡</sup>Also at the Università di Perugia, I-06100, Perugia, Italy.

W. Fetscher, H. J. Gerber, and K. F. Johnson, Phys. Lett. B 173, 102 (1986).

<sup>[2]</sup> R. M. Barnett et al., Phys. Rev. D 54, 251 (1996).

<sup>[3]</sup> Y. S. Tsai, Phys. Rev. D 4, 2821 (1971).

<sup>[4]</sup> Defined as  $A_\ell = 2\nu_\ell/a_\ell/[1+(\nu_\ell/a_\ell)^2]$ , where  $\nu_\ell/a_\ell$  is the ratio between the effective  $Z^0$  vector and axialvector couplings to the leptons. We assume lepton universality in the neutral current and the SLD value  $A_\ell = 0.1543 \pm 0.0039$  is used. See SLD Collaboration, K. Abe *et al.*, Phys. Rev. Lett. **78**, 2075 (1997).

<sup>[5]</sup> ALEPH Collaboration, D. Buskulic *et al.*, Phys. Lett. B 321, 168 (1994); 346, 379 (1995).

<sup>[6]</sup> CLEO Collaboration, J. Bartelt et al., CLEO-CONF-94-21, 1994; R. Ammar et al., Report No. CLNS-96-1429, 1996; T.E. Coan et al., Report No. CLNS-96-1450A, 1997.

<sup>[7]</sup> L3 Collaboration, M. Acciarri *et al.*, Phys. Lett. B 377, 313 (1996).

<sup>[8]</sup> ARGUS Collaboration, H. Albrecht *et al.*, Phys. Lett. B 337, 383 (1994); 341, 441 (1995); 349, 576 (1995).

- [9] ARGUS Collaboration, H. Albrecht *et al.*, Z. Phys. C 58, 61 (1993).
- [10] OPAL Collaboration, R. Akers *et al.*, Z. Phys. C **67**, 45 (1995); K. Ackerstaff *et al.*, Report No. CERN-PPE/97-020 1997
- [11] J.E. Brau and G.J. Tarnopolsky, Phys. Rev. D 24, 2521 (1981).
- [12] A. Rougé, Z. Phys. C 48, 75 (1990).
- [13] M. Davier et al., Phys. Lett. B 306, 411 (1993).
- [14] L. Michel, Proc. Phys. Soc. A 63, 514 (1950); C. Bouchiat and L. Michel, Phys. Rev. 106, 170 (1957).
- [15] SLD Collaboration, K. Abe *et al.*, Phys. Rev. D **52**, 4828 (1995); Nucl. Instrum. Methods Phys. Res., Sect. A **343**, 74 (1994).

- [16] S. Jadach, B.F.L. Ward, and Z. Was, Comput. Phys. Commun. 79, 503 (1994).
- [17] The leptonic charged weak interactions for e and  $\mu$  have been measured with sufficient precision to exclude interactions different from a pure V-A at the  $\ell\overline{\nu}_\ell$  vertex [1,2]. Therefore, one can assume V-A at the  $\ell\overline{\nu}_\ell$  vertex and allow a combination of V-A and V+A at the  $\nu_\tau\tau$  vertex [18]. This assumption reduces the number of free parameters to one as in the hadronic decay channels. In this case the relations between  $h_{\nu_\tau}$  and  $\rho$ ,  $\xi$ ,  $\delta\xi$  are the following:  $h_{\nu_\tau} = 1 \frac{8}{3}\rho = \xi 2 = 1 \frac{8}{3}\delta\xi$ ;  $\eta = 0$ .
- [18] P. Privitera, Phys. Lett. B 288, 227 (1992).